Theoretical photoionization spectra for Mg-isoelectronic Cl^{5+} and Ar^{6+} ions

2015 J. Phys. B: At. Mol. Opt. Phys. 48 105004

(http://iopscience.iop.org/0953-4075/48/10/105004)

IOP Publishing Journal of Physics B: Atomic, Molecular and Optical Physics

J. Phys. B: At. Mol. Opt. Phys. **48** (2015) 105004 (11pp) doi:10.1088/0953-4075/48/10/105004

Theoretical photoionization spectra for Mg-isoelectronic Cl^{5+} and Ar^{6+} ions

Dae-Soung Kim[1] **and Duck-Hee Kwon**[2]

[1] Department of Global Education, Gyeonggi College of Science and Technology, Siheung, Jungwang-Dong 2121-3, Gyonggi-Do 429-792, Republic of Korea
[2] Nuclear Data Center, Korea Atomic Energy Research Institute, Daejeon 305-600, Republic of Korea

E-mail: dskim@gtec.ac.kr

Received 20 November 2014, revised 24 February 2015
Accepted for publication 2 March 2015
Published 15 April 2015

Abstract

Autoionizing resonant structures of Mg-isoelectronic Cl^{5+} and Ar^{6+} ions for the removal of a $3s$ or $3p$ electron from initial $3s^2\ ^1S^e$ and $3s3p\ ^{3,1}P^o$ states have been studied using the eigenchannel R-matrix approach connected with multichannel quantum-defect theory (MQDT) at the R-matrix boundary. The resonant states are verified and analyzed using eigenphase gradients to get resonance locations E_r, effective quantum numbers n^*, and widths Γ_r. It is noted that there are no former theoretical and experimental studies for photoionization cross sections of Mg-isoelectronic Cl^{5+} to compare with ours. For the Mg-isoelectronic Ar^{6+} ion, our calculated ionization thresholds are in good agreement with NIST data and Opacity Project (OP) results. The current photoionization cross sections for the Mg-isoelectronic Ar^{6+} ion are in general agreement with the OP results, except for resonance energy shifts and structures of a few resonances.

Keywords: photoionization, Rydberg series, quantum defect

(Some figures may appear in colour only in the online journal)

1. Introduction

Over the past few decades, there has been much interest in photoionization studies of atoms or ions to understand electron correlations caused by two interacting outer, valence electrons. After He and Be atoms, Mg atoms and Mg-isoelectronic ions are the next simple atomic systems with two valence electron outside the frozen core. Furthermore, photoionization cross sections of Mg and Mg-isoelectronic ions are also important for modeling of astrophysical plasma surrounded by hot radiation sources such as the Sun and stellar transition regions [1].

The autoionizing resonances begin immediately above the ionization threshold. Measurements of these resonances for Mg atoms have been formed in 1969 by Mehlman-Balloffet and Esteva [2]. Other high-resolution experiments have been carried out by several researchers [3–11]. Measurements of absolute photoionization spectra for Mg-isoelectronic Al^+ and Si^{2+} ions have been carried out by West *et al* [12] and Sayyad *et al* [13]. On the other hand, the first calculation for photoionization spectra of a Mg atom was performed by Bates and Altick in 1973 [14], and the characteristics of Mg-isoelectronic series have attracted a great deal of interest theoretically [15–30]. In particular, the Opacity Project (OP) team [31] have performed a number of remarkable theoretical works. The approach developed by the OP team rest on a new formalism of the equation of state [32] and on the computation by *ab initio* methods of precise atomic properties such as energy levels, f-values and photoionization cross sections [33–35].

As a part of the work for Mg isoelectronic sequence, we extended the preceding work for the Mg-isoelectronic S^{4+} ion [29] to Mg-isoelectronic Al^+ [28] and Si^{2+} ions [30], and here report the cross sections for photoionization of the Mg-isoelectronic Cl^{5+} and Ar^{6+} ions for photon-energy ranges from the first $3s$ threshold to the $4s$ threshold, using the non-

Table 1. Semiempirical parameters[a] for effective model potential.

Ion	l	α_1^l	α_2^l	α_3^l	r_c^l
Cl^{5+} $\alpha_{cp} = 0.05093$	$\geqslant 0$	5.21229	16.52851	20.15775	0.3
Ar^{6+} $\alpha_{cp} = 0.03710$	$\geqslant 0$	6.11454	6.28177	6.35079	0.25

[a] See equation (5) in the text.

iterative variational R-matrix method [26]. Photoionization processes considered are as following,

$$A\left(3s^2\right)^1S^e + \hbar\omega \rightarrow A^*(3lnl')^1P^o, \quad \searrow \left[A^+(3l) + e^-(\epsilon l')\right]\ ^1P^o \tag{1}$$

$$A\,(3s3p)^{3,1}P^o + \hbar\omega \rightarrow A^*(3lnl')^{3,1}S^e,\ P^e,\ D^e, \quad \searrow \left[A^+(3l) + e^-(\epsilon l')\right]^{3,1}S^e,\ P^e,\ D^e \tag{2}$$

where A and $\hbar\omega$ represent the Mg-isoelectronic ions and the photon energy, respectively. $A^*(3lnl')(n \geqslant 3)$ is considered as the possible doubly-excited states.

2. Calculational description

The general detailed descriptions for the calculation are given in [17, 36]. The major approximation in the calculation concerns the adoption of a non-relativistic Hamiltonian of the two valence electrons outside the frozen inner shell $1s^22s^22p^6$ electrons [29],

$$H = H(r_1) + H(r_2) + \frac{1}{r_{12}}, \tag{3}$$

where $H(r) = -\frac{1}{2}\nabla^2 + U(r)$ describes the one-electron Hamiltonian. The wave functions of the outer two electrons are represented by the independent-particle wave function

$$\left[-\frac{1}{2}\frac{d^2}{dr^2} + \frac{l(l+1)}{2r^2} + U(r) - E_{nl}\right]\phi_{nl}(r) = 0, \tag{4}$$

where $U(r)$ represents the effective potential for the $e - A^{2+}$ interaction. We have applied the potential form [37]

$$U(r) = -\frac{1}{r}\left[2 + (Z-2)e^{-\alpha_1^l r} + \alpha_2^l\, re^{-\alpha_3^l r}\right] - \frac{\alpha_{cp}}{2r^4}\left[1 - e^{-\left(r/r_c^l\right)^6}\right], \tag{5}$$

where Z and α_{cp} represent nuclear charge and the experimental dipole polarizability [38], respectively. The values of α_i^l and r_c^l given in table 1 are the parameters optimized so that the calculated energy eigenvalues taken from the potential correspond to the experimental energies of Cl^{7+} and Ar^{8+}. The above, sophisticated l-dependent potentials in equation (5) have been applied successfully to several ionic valence energy spectra [37, 39, 40].

Table 2. Related channels up to the energy of the 4s threshold for the ground state of Cl^{7+} and Ar^{8+} ions.

Threshold	Closed channel	Open channel
3s ^{2S}	3snp	
3p ^{2P}	3pns, 3pnd	3skp
3d ^{2D}	3dnp, 3dnf	3skp, 3pks, 3pkd
4s ^{2S}	4snp	3skp, 3pks, 3pkd, 3dkp, 3dkf

Using equation (4), a basis set of the lowest eighteen orbitals for each $n(l \leqslant 3)$, ϕ_{nl}^c, which disappear at the R-matrix surface, is obtained. Furthermore, the lowest two positive energy functions for each l are produced, ϕ_{nl}^o, whose derivatives disappear at the boundary, and they are put into the basis set. We have used $r_0 = 9$ a.u. and $r_0 = 7$ a.u., respectively, for the current calculations of Cl^{5+} and Ar^{6+} ions.

The convergence tests for cross sections have been performed for the ground $3s^2\ ^1S$ state with the five, ten, fifteen and twenty closed orbitals for each $n(l \leqslant 3)$. It is found that convergence could not be achieved with the five and ten closed orbitals, but convergence is good with the fifteen and twenty closed orbitals. Thus, we have used eighteen closed and two open orbitals for each l. Good numerical convergence of orthonomalities for the closed orbitals is achieved in the present calculation, with an accuracy of 10^{-8} or better. A LS coupled two-electron orbital is given by [37]

$$\psi = \sum_{n_1,n_2} c_{n_1n_2} y_{n_1n_2} \tag{6}$$

where $y_{n_1n_2}$ can be represented by,

$$y_{n_1,n_2} = \frac{1}{\sqrt{2}}\left[\frac{\Phi_{n_1}(r_1, \Omega_1, \Omega_2)}{r_2}\phi_{n_2l_2}(r_2) + (-1)^a\frac{\Phi_{n_1}(r_2, \Omega_2, \Omega_1)}{r_1}\phi_{n_2l_2}(r_1)\right], \tag{7}$$

where $a \equiv l_1 + l_2 - L + S$ and

$$\Phi_{n_1}(r_1, \Omega_1, \Omega_2) = \frac{\phi_{n_1l_1}(r_1)}{r_1}Y_{l_1l_2LM}(\Omega_1, \Omega_2). \tag{8}$$

The channel functions Φ_n are for the ionic states incorporating the angular parts of both electrons. Then, the calculations for matrix elements of the one-electron Hamiltonian $H(r)$ are easy since the basis set equation (7) are the eigenfunctions of $H(r_1) + H(r_2)$. Meanwhile, the estimation of matrix elements for $1/r_{12}$ is relatively complicated, but needs to be estimated only once, because our basis set is energy independent. In the current calculations, the set of energy-independent orbitals given in table 2 have been applied for the ground state of Cl^{7+} and Ar^{8+} ions.

Table 3. Ionization thresholds (in eV) of Mg-isoelectronic Cl^{5+} and Ar^{6+} ions.

States	Cl^{5+}	$3s\ ^2S$	$3p\ ^2P$	$3d\ ^2D$	$4s\ ^2S$
$3s^2\ ^1S^e$	Present	96.653	112.058	132.625	154.134
	NIST [41]	96.652	112.079	132.635	154.181
$3s3p\ ^3P^o$	Present	84.260	99.666	120.233	151.742
	NIST [41]	84.260	99.687	120.243	151.789
$3s3p\ ^1P^o$	Present	78.495	93.900	114.468	135.976
	NIST [41]	78.495	93.922	114.477	136.024
	Ar^{6+}				
$3s^2\ ^1S^e$	Present	123.718	140.534	164.491	194.796
	OP [34]	123.528	148.497	171.546	202.081
	NIST [41]	123.718	141.340	164.968	195.128
$3s3p\ ^3P^o$	Present	110.046	126.861	150.818	181.124
	OP [34]	109.685	134.654	157.703	188.239
	NIST [41]	110.045	127.667	151.295	181.455
$3s3p\ ^1P^o$	Present	103.659	120.148	144.431	174.737
	OP [34]	102.396	127.365	150.414	180.950
	NIST [41]	103.659	121.281	144.908	175.069

Beyond the R-matrix volume, the continuum wave function obeys

$$F_{i,\beta}(r) = \left\langle \phi_i \mid \psi_\beta \right\rangle, \quad r \geqslant r_0,$$
$$F'_{i,\beta}(r) = \left\langle \phi_i \mid \frac{\partial \psi_\beta}{\partial r} \right\rangle, \quad r = r_0, \tag{9}$$

where ϕ_i describes the ionic states after one electron goes to a continuum state. The matrices I and J are estimated by using the Wronskian of both sides of equation (9).

$$I_{i,\beta} = \frac{W\left[g_i, F_{i,\beta}(r_0)\right]}{W\left(g_i, f_i\right)},$$
$$J_{i,\beta} = \frac{W\left[f_i, F_{i,\beta}(r_0)\right]}{W\left(g_i, f_i\right)}. \tag{10}$$

The continuum wave functions of the photoelectron are represented by a linear combination of the energy-normalized regular and irregular Coulomb functions f and g [42],

$$F_{i,\beta}(r_0) = f_i(\epsilon_i, r_0) I_{i,\beta} - g_i(\epsilon, r_0) J_{i,\beta},$$
$$F'_{i,\beta}(r_0) = \frac{\partial}{\partial r} f_i(\epsilon, r_0) I_{i,\beta} - \frac{\partial}{\partial r} g_i(\epsilon, r_0) J_{i,\beta}, \tag{11}$$

where $\epsilon_i = E - E^i_{ion}$ is the electron energy relative to the ionization threshold of the ith channel. The reaction matrix $K = JI^{-1}$ can be diagonalized as

$$U^T K U = \tan \pi\mu, \tag{12}$$

and we get the eigenvalues $\tan(\pi\mu_\alpha)$ and the eigenvectors U_α. The eigenstates of the short-range reaction matrix $\psi_\alpha = \sum_{\beta,i} \psi_\beta (I^{-1})_{\beta i} U_{i\alpha} \cos(\pi\mu_\alpha)$ have the following asymptotic form

$$\psi_\alpha = \sum_i \phi_i \Big[f_i(\epsilon_i, r) U_{i\alpha} \cos(\pi\mu_\alpha) - g_i(\epsilon_i, r) U_{i\alpha} \sin(\pi\mu_\alpha) \Big], \quad r \geqslant r_0. \tag{13}$$

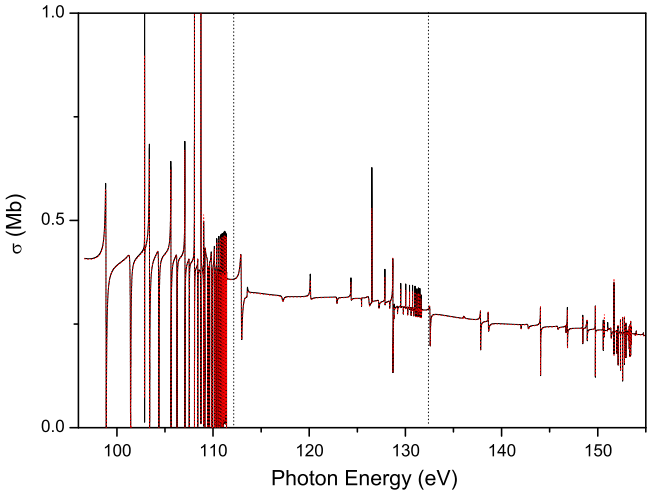

Figure 1. Calculated photoionization cross sections for the ground-state of Cl^{5+} ion up to the Cl^{6+} $4s$ threshold energy. Black solid line is for length gauge result and red dotted line is for velocity gauge result. The $3p$ and $3d$ thresholds are shown by the up-and-down dotted lines.

These energy-normalized eigenstates are connected to the reduced dipole matrix elements in the length and velocity form as

$$d_\alpha(L) = \left\langle \psi_0 \| \vec{r}_1 + \vec{r}_2 \| \psi_\alpha \right\rangle$$
$$d_\alpha(V) = \frac{1}{\omega} \left\langle \psi_0 \| \vec{\nabla}_1 + \vec{\nabla}_2 \| \psi_\alpha \right\rangle, \tag{14}$$

respectively, where ψ_0 represents the ground-state wavefunction. The $N_o \times N_o$ open-channel reaction matrix is written as

$$K^{oo}_{phys} = K^{oo} - K^{oc} \Big[K^{cc} + \tan \pi n^* \Big]^{-1} K^{co}, \tag{15}$$

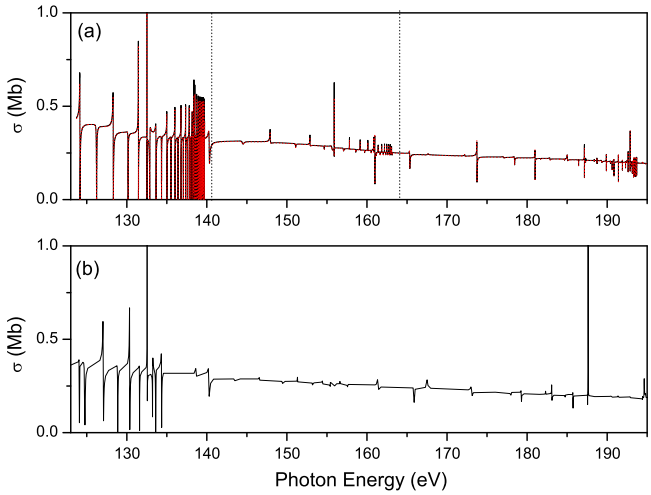

Figure 2. (a) Calculated photoionization cross sections for the ground-state of Al^{6+} ion up to the Ar^{7+} 4*s* threshold energy. Black solid line is for length gauge result and red dotted line is for velocity gauge result. The 3*p* and 3*d* thresholds are shown by the up-and-down dotted lines, (b) OP results [34].

where the effective quantum number in the closed channels is given by

$$n^* = \frac{Z - z}{\sqrt{2(E_t - E_r)}}, \tag{16}$$

where Z and z are the atomic number and the number of electrons in the final ion, respectively. E_t and E_r are the threshold and the corresponding resonance energy, respectively. The eigenphase in each channel i is defined as

$$\delta_i = \tan^{-1}\lambda_i, \quad i = 1, \ldots, N_o, \tag{17}$$

where λ_i is the eigenvalue of K^{oo}_{phys}. A resonance position E_r can be defined as the energy at which the eigenphase sum δ has its maximum value of $d\delta/dE$. The width of the resonance Γ_r is related to the inverse of the eigenphase gradient,

$$\Gamma_r = 2\left(\frac{d\delta}{dE}\right)^{-1}_{E=E_r}. \tag{18}$$

The associated dipole matrix element is represented by

$$d^o_{phys} = d^o_\alpha - d^c_\alpha\left[K^{cc} + \tan \pi n^*\right]^{-1} K^{co}, \tag{19}$$

where d^o_α and d^c_α are the reduced matrix elements given in equation (15) corresponding to open and closed channels, respectively. Then, the partial photoionization cross section is represented by

$$\sigma_i = \frac{4\pi^2\alpha}{3}\omega|d_i^{(-)}|^2 \tag{20}$$

in a.u., where α is the fine structure constant and

$$d_i^{(-)} = \frac{d^o_{phys}}{1 + iK^{oo}_{phys}} \tag{21}$$

Table 4. Resonance parameters n^*, E_r (in eV), and Γ_r(in eV) for the photoionization processes $^1S \rightarrow {}^1P^o$.

		Cl^{5+}			Ar^{6+}		
States	n	n^*	E_r	Γ_r	n^*	E_r	Γ_r
$3pns\ ^1P$	7	6.744	101.424	0.207	6.337	124.150	0.091
	8	7.462	103.395	0.090	7.320	128.307	0.117
	9	8.636	105.625	0.052	8.466	131.449	0.037
	10	9.786	107.077	0.030	9.690	133.650	0.092
$3pnd\ ^1P$	6	6.065	98.874	0.173	6.775	126.226	0.196
	7				7.935	130.160	0.105
	8	7.910	104.363	0.133	8.999	132.518	
	9	9.082	106.254	0.069	10.197	134.338	0.072
	10	10.246	107.527	0.036			
$3dnd\ ^1P$	5	4.567	109.151	0.073	4.592	132.874	0.137
	6	5.645	117.253	0.601	5.772	144.481	0.738
	7	6.258	120.119	0.175	6.341	147.909	0.227
	8	7.691	124.345	0.092	7.579	152.885	0.108
	9	8.751	126.229	0.513	8.670	155.623	0.530
	10	9.542	127.245	0.236	9.619	157.286	
$3dnf\ ^1P$	5	5.068	113.559	0.206	5.016	137.991	
	6				5.823	144.825	0.030
	7	7.091	122.883	0.240	7.054	151.091	0.243
	8	8.260	125.446	0.049	8.238	154.669	0.056
	9	8.957	126.520	0.007	8.907	156.087	
	10	10.153	127.873	0.031	9.991	157.813	0.035

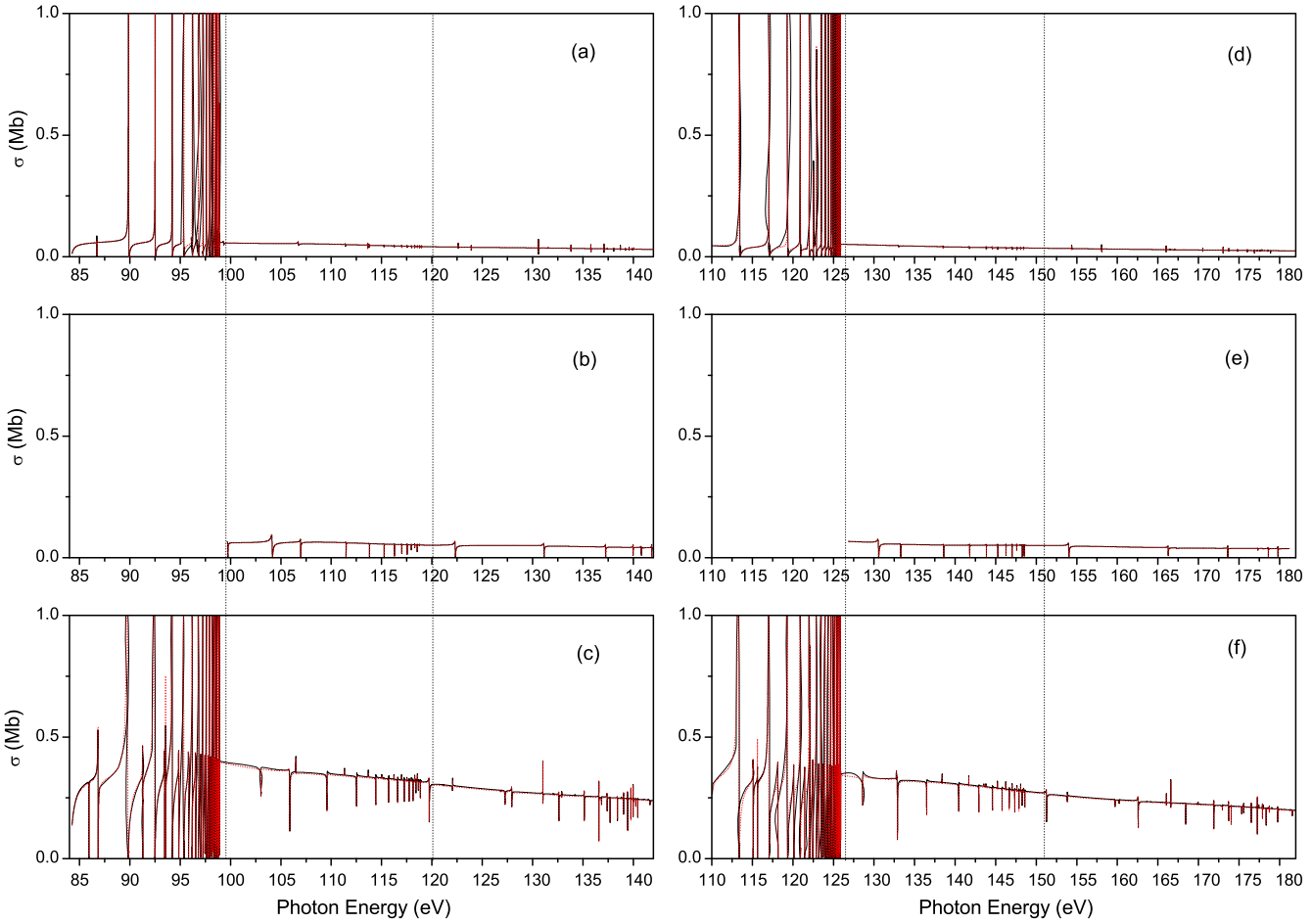

Figure 3. Calculated photoionization cross sections for the $3s3p\ ^{3P}$ state: cross sections (a) for the process $^3P^o \rightarrow {}^3S$ of the Cl^{5+} ion, (b) for the process $^3P^o \rightarrow {}^3P$ of the Cl^{5+} ion, (c) for the process $^3P^o \rightarrow {}^3D$ of the Cl^{5+} ion, (d) for the process $^3P^o \rightarrow {}^3S$ of the Ar^{6+} ion, (e) for the process $^3P^o \rightarrow {}^3P$ of the Ar^{6+} ion, (f) for the process $^3P^o \rightarrow {}^3D$ of the Ar^{6+} ion. Black solid line is for length gauge result and red dotted line is for velocity gauge result. The $3p$ and $3d$ thresholds are shown by the up-and-down dotted lines.

is the outgoing dipole matrix element. The total photoionization cross section is given by

$$\sigma = \frac{4\pi^2\alpha}{3}\omega\sum_i |d_i^{(-)}|^2. \tag{22}$$

The general details of the eigenchannel R-matrix method can be found elsewhere [16, 36, 37].

3. Results and discussions

The ionization energies (in eV) of the Cl^{6+} and Ar^{7+} $3\,l$ thresholds relative to the initial ground ^1S and excited $^{3,1}P$ states of Mg-isoelectronic Cl^{5+} and Ar^{6+} ions are listed in table 3. The energies of NIST data [41] shown in table 3 have been averaged by $\sum_J (g_J E_J)/\sum_J g_J$, where g_J represents the statistical weight for J state. The agreement of energies between our results and NIST data is reasonably good, however the OP results [34] for Ar^{6+} ions show some differences. For the Cl^{5+} ion, there are no available OP results.

3.1. Photoionization from the ground $3s^2\ ^1S$ state of Mg-isoelectronic Cl^{5+} and Ar^{6+} ions

The results of the present total photoionization cross sections from the ground-state of Mg-isoelectronic Cl^{5+} and Ar^{6+} ions are shown in figures 1 and 2, respectively, as a function of photon energy. The excellent agreement between length (black solid curve) and velocity (red dotted curve) results manifests the degree of accuracy for the present calculations. As far as we know, there are no available previous results to compare with our results for the Mg-isoelectronic Cl^{5+} ion, while the present results of total photoionization cross section for the Mg-isoelectronic Ar^{6+} ion are compared with the earlier OP results [34]. The OP results for the Ar^{6+} ion are shifted to a lower energy by about 0.2 eV compared with the present results. However, there are some significant differences in the structure of the resonance shapes between the present and OP results for the Ar^{6+} ion. For example, the first single resonance just above the $3s$ threshold represents the $3p7s\ ^1P$ resonance in the present result, but the OP result shows an overlap with the other resonances. While the databank of OP works for Ar^{6+} ion [34] do not have enough very-small energy points, we have used the very small energy intervals $\Delta E = 0.002$ eV in our calculations.

Table 5. Resonance parameters n^*, E_r (in eV), and Γ_r(in eV) for the photoionization processes $^3P^o \rightarrow {}^3S,{}^3P,{}^3D$.

		Cl^{5+}			Ar^{6+}		
States	n	n^*	E_r	Γ_r	n^*	E_r	Γ_r
$3pnp\ ^3S$	6	5.724	84.716				
	7	6.632	88.529				
	8	7.651	91.296		7.335	114.469	
	9	8.847	93.407		8.652	117.954	
	10	9.473	94.207	0.029	9.425	119.356	0.047
$3dnd\ ^3S$	5	4.514	96.159				
	6	6.023	106.734	0.002	6.124	133.042	0.167
	7	6.958	110.118		7.096	137.581	
	8	8.612	113.630	0.006	7.665	139.470	
	9	8.700	113.763		8.576	141.754	0.058
	10	9.905	115.241	0.002	9.768	143.831	0.043
$3dnd\ ^3P$	6	5.515	104.130	0.224	5.738	130.569	0.241
	7				6.362	134.348	
	8	7.479	111.477	0.003	7.617	139.325	
	9	8.723	113.795	0.001	8.596	141.795	0.025
	10	9.926	115.262	0.001	9.783	143.852	0.007
$3pnp\ ^3D$	6	5.971	85.930				
	7	6.739	88.880				
	8	7.639	91.273	0.037	7.529	115.100	0.062
	9	8.882	93.456	0.033	8.751	118.155	0.036
	10	9.456	94.188	0.039	9.402	119.319	0.046
$3pnf\ ^3D$	6	5.973	85.936	0.059			
	7	7.034	89.765	0.135	7.005	113.274	0.121
	8	8.223	92.423	0.083	8.227	117.011	0.063
	9	8.953	93.555	0.009	8.760	118.173	
	10	10.087	94.852	0.023	9.942	120.117	0.026
$3dns\ ^3D$	4	3.779	85.929	0.003			
	5	4.436	95.346	0.030	4.320	115.092	0.099
	6	5.336	103.030	0.014	5.342	127.456	
	7	6.548	108.811		6.686	135.905	
	8	7.410	111.313	0.005	7.325	138.393	0.025
	9	8.649	113.687	0.007	8.543	141.684	0.019
	10	9.688	115.015	0.099	9.570	143.539	0.124
$3dnd\ ^3D$	4	3.830	86.843	0.070			
	5	4.805	99.018		5.004	124.190	0.008
	6	5.841	105.879	0.094	6.074	132.748	0.063
	7	6.780	109.580		6.823	136.496	0.061
	8	7.968	112.520	0.002	7.811	139.892	
	9	9.181	114.424	0.008	9.190	142.925	
	10	9.865	115.202	0.016	9.740	143.790	0.018

Thus, present results represent more rich resonance structures than the OP results.

In the energy region below the Cl^{6+} and Ar^{7+} $3p$ thresholds, we expect the two doubly-excited states, $3pns\ ^1P$ and $3pnd\ ^1P$, converging to each of the $3p$ threshold. However, $3pns\ ^1P$ ($n \leqslant 6$) and $3pnd\ ^1P$ ($n \leqslant 5$) appeared as real bound states for each of the Mg-isoelectronic Cl^{5+} and Ar^{6+} ions in the present calculations. The perturbers converging to the each of the $3d$ or $4s$ thresholds have significant effects on the $3pns\ ^1P$ and $3pnd\ ^1P$ resonances as shown in table 4.

The intermixing among the resonances converging to the various $n = 3$ and $n = 4$ final ionic states is much greater for Cl^{5+} and Ar^{6+} than for Mg [26], Al^+ [27], Si^{2+} [30], and S^{4+} [29], resulting in much more complicated forms of resonances. These occur because energy magnitude of the resonance series converging to each threshold increases with Z much more quickly than the energy gap of the thresholds [43]. This leads to the significant result that the resonance structure is even more complicated for photoionization of Mg-isoelectronic Cl^{5+} and Ar^{6+} ions. This is clear from table 4 where the details of the resonant series converging on

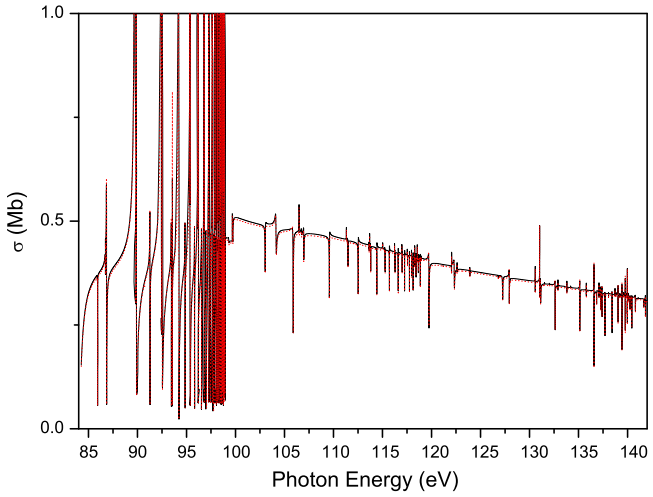

Figure 4. Present total photoionization cross sections from the initial $3s3p\ ^3P^o$ state of the Cl^{5+} ion to the Cl^{6+} $4s$ threshold. Black solid line is for length gauge result and red dotted line is for velocity gauge result.

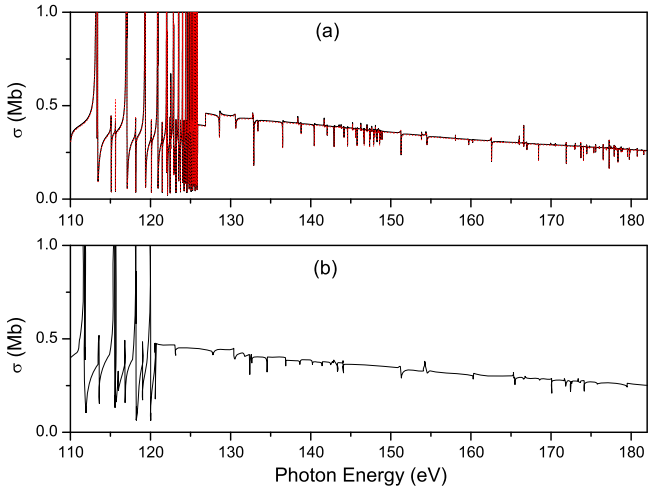

Figure 5. (a) Present total photoionization cross sections from the initial $3s3p\ ^3P^o$ state of the Ar^{6+} ion to the Ar^{7+} $4s$ threshold. Black solid line is for length gauge result and red dotted line is for velocity gauge result, (b) OP results [34].

the $3p$ threshold are listed and quite a number of irregularities are seen in the quantum defects and widths in the resonances owing to perturbers from the lower members of series converging to $3d$ and $4s$ thresholds. Especially, it appears that these perturbers lie between the $n = 12$ and $n = 13$ resonance series. Owing to these perturbers, the $3pns\ ^1$P and $3pnd\ ^1$P series converging to the $3p$ threshold do not have smooth regular behavior with approximately steady quantum defects even at $n = 10$, as seen in table 4.

Analogously, the predicted resonances converging to each of the $3d$ thresholds for the Cl^{5+} and Ar^{6+} ions are the $3dnd\ ^1$ P and $3dnf\ ^1$ P series. These autoionizing resonance series are also disordered by the effects of perturbers that converge to higher thresholds than $3d$ thresholds. Some of these perturbers are embedded below the $n = 10$ resonance. For instance, it appears that the perturbers lie at $E = 120.171$ eV, 126,370 eV, and 127.314 eV for the Cl^{5+} ion. On the other hand, a bunch of perturbers at $E = 140.273$ eV, 140.294 eV, 140.307 eV, and 157.069 eV lie below the $n = 10$ resonance. Thus, a number of anomalies are seen as in table 4.

3.2. Photoionization from the initial $3s3p\ ^3$P *state of Mg-isoelectronic* Cl^{5+} *and* Ar^{6+} *ions*

The photoionization cross sections from the initial $3s3p\ ^3$P states of Mg-isoelectronic Cl^{5+} and Ar^{6+} ions have been calculated in the energy region from the first ionization threshold to the each of the $4s$ thresholds. The channel cross sections associated with the equations (2) for photoionization of the $3s3p^3P^o$ state of the Mg-isoelectronic Cl^{5+} and Ar^{6+} ions are shown in figures 3(a)–(c) and 3(d)–(f), respectively.

The autoionizing resonances series also show very complicated and irregular forms. The autoionizing ^{3}S, ^{3}P, and ^{3}D resonance series converging to the ionic Cl^{6+} and Ar^{7+} $3p$, for instance, are interrupted by some perturbers series that converge to the Cl^{6+} and Ar^{7+} $3d$, $4s$ and even higher thresholds, as shown in the figures 3(a)–(c) and 3(d)–(f), respectively. The lower members of these resonances have been studied in detail and their energy positions E_r, effective quantum numbers n^*, and widths Γ_r are given in table 5.

It is noted that the $3pnp\ ^3$S and ^{3}D ($n \leqslant 5$ for the Cl^{5+}, $n \leqslant 7$ for the Ar^{6+}) states appear as real bound states in our calculations. Among the $3pnp\ ^3$S series, the perturbers lie at $E = 86.724$ eV, 89.868 eV, and 92.512 eV for the Cl^{5+} ion, and at $E = 117.056$ eV for the Ar^{6+} ion. In the $3pnp\ ^3$D series, the perturbers are embedded at $E = 85.936$ eV and 115.631 eV for the Cl^{5+} and Ar^{6+} ions, respectively. Another perturber in the $3pnf\ ^3$D series lies at $E = 86.843$ eV for the Cl^{5+} ion. In the case of the $3dnd\ ^3$S series, the $3dnd\ ^3$S ($n \leqslant 4$ for the Cl^{5+}, $n \leqslant 5$ for the Ar^{6+}) states appear as real bound states. Other perturbers are embedded at $E = 105.810$ eV, 111.409 eV, and 113.661 eV for the Cl^{5+} ion, and $E = 131.572$ eV, 138.511 eV for the Ar^{6+} ion. Among the $3dnd\ ^3$P series, the perturbers lie at $E = 106.967$ between the $n = 6$ and $n = 7$ for the Cl^{5+} ion, while the perturbers lie at $E = 133.293$ eV, 141.134 eV, 142.586 eV for the Ar^{6+} ion. The autoionizing resonance series in the $3s3p\ ^3P^o \rightarrow ^3$ D process represent more complicated forms than the ^{3}S and the ^{3}P processes owing to having had more resonances included: $3pnp$, $3pnf$, $3dns$, and $3dnd$.

The autoionizing Rydberg series $3dns\ ^3$D and $3dnd\ ^3$D converging to the $3d$ thresholds are also affected by a large number of perturbers. In the $3dns\ ^3$D series, the perturbers lie at $E = 105.293$ eV for the Cl^{5+} ion, and at $E = 115.631$ eV, 128.618 eV, 129.677 eV, 131.781 eV, and 138.802 eV for the Ar^{6+} ion. In the $3dnd\ ^3$ series, the perturbers lie at $E = 89.757$ eV, 106.005 eV, 106.486 eV, and 115.198 eV for the Cl^{5+} ion, and at $E = 132.889$ eV, 133.813 eV, 137.099, and 140.452 eV for the Ar^{6+} ion.

All of these perturbers push and pull the energy positions of the primitive Rydberg series unlike the Mg atom [26], and

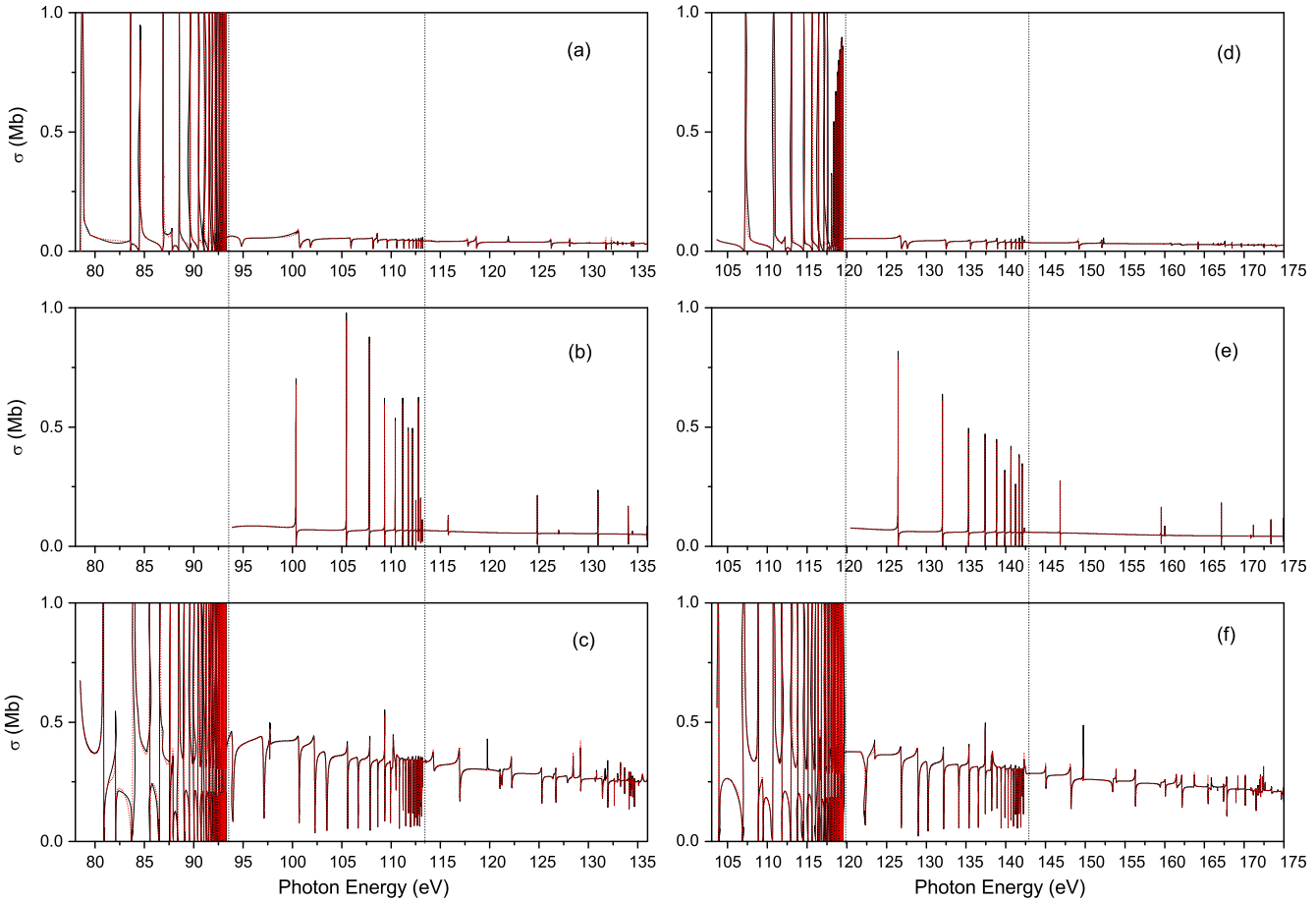

Figure 6. Calculated photoionization cross sections for the $3s3p\,^1P$ state: cross sections (a) for the process $^1P^o \rightarrow {}^1$S of the Cl^{5+} ion, (b) for the process $^1P^o \rightarrow {}^1$P of the Cl^{5+} ion, (c) for the process $^1P^o \rightarrow {}^1$D of the Cl^{5+} ion, (d) for the process $^1P^o \rightarrow {}^1$S of the Ar^{6+} ion, (e) for the process $^1P^o \rightarrow {}^1$P of the Ar^{6+} ion, (f) for the process $^1P^o \rightarrow {}^1$D of the Ar^{6+} ion. Black solid line is for length gauge result and red dotted line is for velocity gauge result. The $3p$ *and* $3d$ thresholds are shown by the up-and-down dotted lines.

sometimes overlap each other, as indicated by the deviations in quantum defects as listed in the table 5.

The present total photoionization cross sections for the photoionization of the $3s3p\,^3$P states of the Cl^{5+} ion are gained by summing up the respective channel cross sections represented in figures 3(a)–(c) and are shown in figure 4. To our knowledge, there is no preceding report for the photoionization cross section of the Mg-isoelectronic Cl^{5+} ion, and this present work is the first report for this ion.

Analogously, the total photoionization cross sections of the $3s3p\,^3$P states of the Ar^{6+} ion are gained by summing up the respective channel cross sections represented in figures 3(d)–(f). The present and the OP results [34] for the total photoionization cross sections of the $3s3p\,^3$P states are shown in figure 5(a) and 5(b), respectively. The OP results show general agreement with the our results for an Ar^{6+} ion. However, some significant inconsistencies are found as shown in figure 5. With movement to a lower energy than our results, the OP results do not have enough energy points. Furthermore, the resonance structures are also different. After the first resonance above the $3s$ threshold, our results have two resonances due to the ^{3}D series, as shown in figure 3(f). However, the OP results have one resonance.

3.3. Photoionization from the initial $3s3p\,^1$P *state of Mg-isoelectronic* Cl^{5+} *and* Ar^{6+} *ions*

The photoionization cross sections from the $3s3p\,^1$P states of Mg-isoelectronic Cl^{5+} and Ar^{6+} ions have been also calculated in the energy region from the ionization threshold to each of the $4s$ thresholds. The channel cross sections associated with equation (2) for the photoionization of the $3s3p\,^1P^o$ state of the Mg-isoelectronic Cl^{5+} and Ar^{6+} ions are shown in figures 6(a)–(c) and 6(d)–(f), respectively.

The autoionizing processes of the singlet $3s3p\,^1$P for the Mg-isoelectronic Cl^{5+} and Ar^{6+} ions also show very complicated and irregular resonance forms as the triplet $3s3p\,^3$P. As shown in figures 6(a)–(c) and 6(d)–(f), the autoionizing ^{1}S, ^{1}P, and ^{1}D resonance series converging to the ionic Cl^{6+} and $Ar^{7+}3p$ threshold are also perturbed by some perturber series that converge to the Cl^{6+} and $Ar^{7+}3d\,4s$, and even higher thresholds. Table 6 gives the lower members of these resonances, their energy positions E_r, effective quantum numbers n^*, and widths Γ_r.

The $3pnp\,^1$S and ^{1}D ($n \leqslant 5$ for the Cl $^{5+}n \leqslant 7$ for the Ar^{6+}) states appear as real bound states in our calculations. The perturbers among the $3pnp\,^1$S series lie at $E = 79.694$ eV and 87.783 eV for the Cl^{5+} ion. The perturbers in the case of

Table 6. Resonance parameters n^*, E_r (in eV), and Γ_r (in eV) for the photoionization processes $^1P^o \rightarrow {}^1S,^1P,^1D$.

		Cl^{5+}			Ar^{6+}		
States	n	n^*	E_r	Γ_r	n^*	E_r	Γ_r
$3pnp\ ^1S$	6	5.674	78.686	0.146			
	7	6.516	82.364				
	8	7.243	84.565	0.153	7.102	107.255	0.171
	9	8.367	86.904	0.105	8.299	110.796	0.103
	10	9.552	88.533	0.046	9.472	113.045	0.065
$3dnd\ ^1S$	4	3.985	83.618				
	5	4.997	94.849	0.862			
	6	5.961	100.685	0.568			
	7	6.222	101.817	0.459			
	8	7.572	105.925	0.245	7.573	108.851	
	9	9.148	108.616	0.119	8.992	112.229	0.174
	10	10.033	109.602	0.109	10.001	113.809	
$3dnd\ ^1P$	6	5.893	100.362	0.012	6.090	16.458	0.014
	7	7.260	105.174				
	8	7.375	105.463	0.008	7.336	132.044	0.010
	9	8.567	107.794	0.007	8.554	135.321	0.003
	10	9.778	109.344	0.005	9.746	137.414	0.002
$3pnp\ ^1D$	7	6.433	82.064	0.073	6.329	103.832	0.154
	8	7.653	85.536	0.036	7.571	108.843	0.067
	9	8.843	87.636	0.018	8.789	111.845	0.045
	10	9.491	88.462	0.153	9.444	112.999	0.077
$3pnf\ ^1D$	7	6.989	83.871	0.210	7.036	107.010	0.123
	8	8.165	86.552	0.049	8.281	110.753	0.168
	9	9.040	87.905	0.173	8.801	111.869	
	10	10.047	89.046	0.021	9.980	113.782	0.033
$3dns\ ^1D$	4	3.817	80.845	0.122			
	5	4.885	93.939	0.348	4.813	115.659	0.026
	6	5.332	97.106	0.429	5.494	122.345	0.478
	7	6.338	102.273	0.235	6.568	128.979	0.264
	8	7.431	105.598	0.088	7.377	132.181	0.096
	9	8.614	107.866	0.053	8.586	135.386	0.052
	10	9.795	109.361	0.015	9.756	137.427	0.035
$3dnd\ ^1D$	4	4.011	83.871	0.210			
	5	5.079	95.479		5.005	117.819	0.010
	6	5.960	100.677	0.195	6.157	126.846	0.200
	7	6.677	103.480	0.402	6.847	130.212	0.318
	8	7.920	106.659	0.125	8.033	134.100	0.148
	9	9.175	108.648	0.071	9.201	136.558	0.097
	10	10.334	109.880	0.003	10.351	138.209	0.106
		10.401	109.939	0.047	10.416	138.287	

the $3dnd\ ^1S$ series lie between the $n = 8$ and $n = 9$ series, at $E = 108.166$ eV for the Cl^{5+} and at $E = 111.567$ eV for the Ar^{6+}, respectively. The $3d8d\ ^1P$ resonance among the $3dnd\ ^1P$ series for the Ar^{6+} ion is overlapped by the effects of the perturbers converging to the higher thresholds. In the autoionizing Rydberg series $3pnp^1D$ for the Ar^{6+} ion, an perturber lies at the $E = 109.448$ eV between $n = 8$ and $n = 9$. In the case of the $3dns^1D$ series, the perturbers lie at $E = 97.705$ eV and 102.938 eV for the Cl^{5+} ion, and at $E = 123.496$ eV for the Ar^{6+} ion. In the $3dnd\,^3D$ series, some of the perturbers lie above the $n = 10$ series for each of the Cl^{5+} and Ar^{6+} ions.

The present total photoionization cross sections for photoionization of the initial $3s3p\,^1P$ states of the Cl^{5+} ion are gained by summing up the respective channel cross sections represented in figures 6(a)–(c), and are shown in figure 7, with no available preceding results to compare with.

The total photoionization cross sections of the initial $3s3p\,^1P$ states of the Ar^{6+} ion are gained by summing up the respective channel cross sections represented in figures 6 (d)–

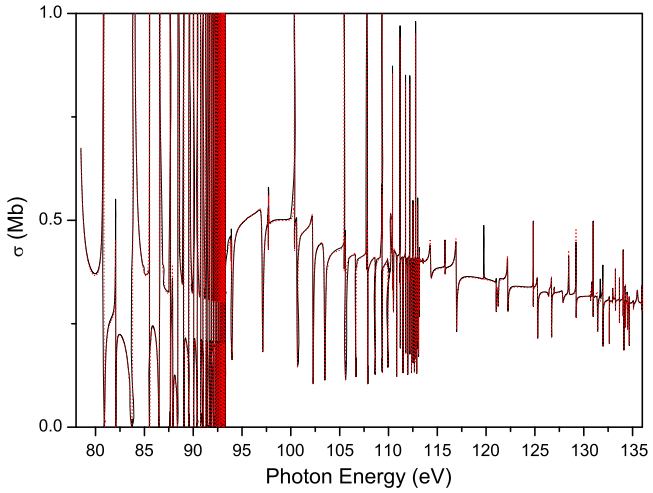

Figure 7. Present total photoionization cross sections from the initial $3s3p\,^1P^o$ state of the Cl^{5+} ion to the Cl^{6+} $4s$ threshold. Black solid line is for length gauge result and red dotted line is for velocity gauge result.

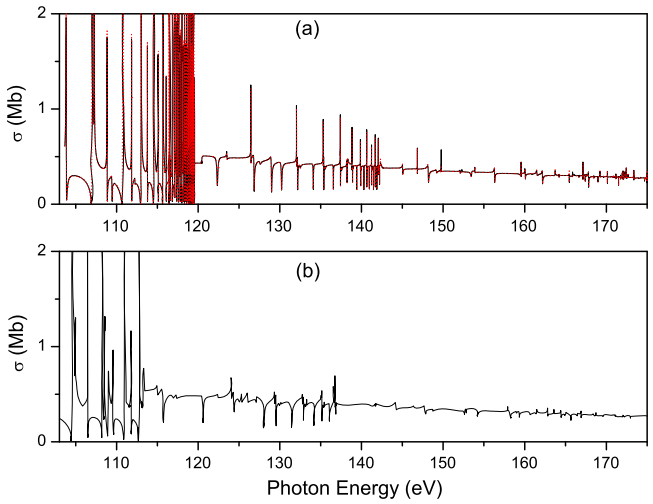

Figure 8. (a) Present total photoionization cross sections from the initial $3s3p\,^1P^o$ state of the Ar^{6+} ion to the Ar^{7+} $4s$ threshold. Black solid line is for length gauge result and red dotted line is for velocity gauge result, (b) OP results [34].

(f). The present and OP results [34] for the total photoionization cross sections of the $3s3p$ ^{1}P states are shown in figure 8(a) and 8(b), respectively. Apart from general agreement between the our results and OP results, some significant inconsistencies are also found, as shown in figure 8. With the shift to a lower energy by about 1.26 eV than our results, the OP results do not show the $3p8p$ ^{1}S resonance that is the first autoionizing state in our results, as shown in figure 8.

4. Conclusions

Calculated results of channel and summed photoionization spectra for the ground $3s^2$ ^{1}S and excited $3s3p$ $^{3,1}P$ states of Mg-isoelectronic Cl^{5+} and Ar^{6+} ions are presented in the energy range from the photo-ionic $3s$ to $4s$ thresholds, adopting a rather efficient non-iterative eigenchannel R-matrix method, which is different from the extensively used iterative R-matrix approach. These are the first photoionization cross-section results for the Mg-isoelectronic Cl^{5+} ion, since there is no preceding theoretical or experimental results to compare with. For Mg-isoelectronic Ar^{6+} ion, preceding OP results are compared with our work. Overall agreement is shown, but there are some energy shifts and non-existence of resonances in the opacity results when compared to our results, in part, owing to coarse energy mesh points in the OP work.

It is noteworthy that for most doubly-excited states converging to the $3p$ and $3d$ thresholds, a lot of members lie below the $3s$ threshold and these interlopers work as perturbers; this takes place since the energy splitting between the $3l$ threshold is small. An accurate analysis and verification of these low-lying autoionizing levels is described; a process made more complex by the overlap of the multiple series converging to different thresholds. However, by employing eigenphase sum gradients, most notable resonances have been clarified.

Since there is no previous experiment to compare with, further experimental measurements would be worthwhile to validate our understanding of the physics of these photoionization phenomena. With the coming of the third-generation synchrotron radiation at present, it is desirable to study for these Mg-isoelectronic $Cl^{5+}$and Ar^{6+} ions utilizing the merged-beam technique [44–48].

To understand the evolution of resonances according to the nuclear charge, further calculations for photo ionization cross section of Mg-isoelectronic phosphorus(P) and analysis of resonance structures for the Mg-isoelectronic sequences, comparing our results for the Be-like sequences [49], will be performed.

Acknowledgments

This research was supported by the National R&D Program through the National Research Foundation of Korea (NRF) funded by the Ministry of Science, ICT & Future Planning.

References

[1] Doschek G A and Feldman U 1987 *Astrophys. J.* **315** L67
[2] Mehlman-Balloffet G and Esteva J-M 1969 *Astrophys. J.* **157** 945
[3] Esteva J-M, Mehlman-Balloffet G and Romand J 1972 *J. Quant. Spectrosc. Radiat. Transfer* **12** 1291
[4] Rassi D, Pejcev V, Ottley T W and Ross K J 1977 *J. Phys. B.: At. Mol. Phys.* **10** 2913
[5] Baig M A and Connerade J P 1978 *Proc. R. Soc.* A **364** 353
[6] Preses M, Burkhardt C E, Garver W P and Leventhal J J 1984 *Phys. Rev.* A **29** R985
[7] Fiedler W, Kortenkamp Ch and Zimmermann P 1987 *Phys. Rev.* A **36** 384

[8] Yih T S, Wu H H, Chan H T, Chu C C and Pong B J 1989 *Chinese J. Phys.* **27** 136
[9] Schinn G W, Dai C J and Gallagher T F 1991 *Phys. Rev.* A **43** 2316
[10] Fung H S, Chu C C, Hsu S J, Wu H H and Yih T S 2000 *Sci. Instrum. Rev.* **71** 1564
[11] Wehlitz R, Lukić D and Juranić P N 2007 *J. Phys. Jpn.* **40** 2385
[12] West J B, Andersen T, Brooks R L, Folkmann F, Kjeldsen H and Knudsen H 2001 *Phys. Rev.* A **63** 052719
[13] Sayyad M H, Kennedy E T, Kiernan L, Mosnier J-P and Costello J T 1995 *J. Phys. B.: At. Mol. Opt. Phys.* **28** 1715
[14] Bates G N and Altick P L 1973 *J. Phys. B.: At Mol. Phys.* **6** 653
[15] Dubau J and Wells J 1973 *J. Phys. B.: At Mol. Phys.* **6** L31
[16] Greene C H 1981 *Phys. Rev.* A **23** 661
[17] O'Mahony P F and Greene C H 1985 *Phys. Rev.* A **31** 250
[18] Rescigno T N 1985 *Phys. Rev.* A **31** 607
[19] Radojević V and Johnson W R 1985 *Phys. Rev.* A **31** 2991
[20] Mendoza C and Zeippen C J 1987 *Astron. Astrophys.* **179** 346
[21] Moccia R and Spizzo P 1988 *J. Phys. B.: At. Mol. Opt. Phys.* **21** 1133
[22] Altun Z 1989 *Phys. Rev.* A **40** 4968
[23] Butler K, Mendoza C and Zeippen C J 1993 *J. Phys. B.: At. Mol. Opt. Phys.* **26** 4409
[24] Chi H-C and Huang K-N 1994 *Phys. Rev.* A **50** 392
[25] Chi H-C 1997 *Phys. Rev.* A **56** 4118
[26] Kim D-S and Tayal S S 2000 *J. Phys. B.: At. Mol. Opt. Phys.* **33** 3235
[27] Kim D-S and Kim Y S 2007 *J. Phys. Soc. Jpn.* **76** 014302
[28] Kim D-S and Kim Y S 2008 *J. Phys. B.: At. Mol. Opt. Phys.* **41** 165002
[29] Kim D-S and Kwon D-H 2013 *Phys. Rev.* A **88** 033426
[30] Kim D-S and Koike F 2008 *J. Phys. Soc. Jpn.* **77** 124302
[31] The Opacity Project Team 1995 *The Opacity Project* Vol 1 (Briston, UK: Institute of Physics Publishing)
[32] Hummer D G and Mihalas D 1988 *Astrophysical. Journal* **331** 794
[33] Seaton M J 1987 *J. Phys. B.: At. Mol. Opt. Phys.* **20** 6363
[34] http://cdsweb.u-strasbg.fr/topbase/topbase.html
[35] Seaton M J, Yan Y, Mihalas D and Pradhan A K 1994 *Mon. Not. R. Astron. Soc.* **266** 805
[36] Greene C H and Jungen C 1985 *Adv. At Mol. Phys.* **21** 51
[37] Aymar M, Greene C H and Luc-Koenig E 1999 *Rev. Mod. Phys* **68** 1015
[38] Johnson W R, Kolb D and Huang K-N 1983 *At. Data Nucl. Data Tables* **28** 333
[39] Aymar M 1990 *J. Phys. B.: At. Mol. Opt. Phys.* **23** 2697
[40] Greene C H and Aymar M 1991 *Phys. Rev.* A **44** 1773
[41] http://www.nist.gov/pml/data/asd.cfm
[42] Seaton M J 1983 *Rep. Prog. Phys.* **46** 167
[43] Chu W C, Zhou H L, Hibbert A and Manson S T 2009 *J. Phys.* B **42** 205003
[44] Kjeldsen H, Folkmann F, Hensen J E, Knudsen H, Rasmussen M S, West J B and Andersen T 1999 *Astron. Astrophys.* **524** L143
[45] Bizau J M *et al* 2000 *Phys. Rev. Lett.* **84** 435
[46] Covington A M *et al* 2001 *Phys. Rev. Lett.* **87** 243002
[47] Champeaux J-P, Bizau J-M, Cubaynes D, Blancard C, Nahar S, Hitz D, Bruncau J and Wuilleumier F J 2003 *Astrophys. J.* **148** 583
[48] Bizau J-M, Champeaux J-P, Cubaynes D, Wuilleumier F J, Folkmann F, Jacobsen T S, Penent F, Blancard C and Kjeldsen H 2005 *Astron. Astrophys.* **439** 387
[49] Kim D-S and Kwon D-H 2013 *J. Phys. B.: At. Mol. Opt. Phys.* **45** 185201